Molecular Therapy
Nucleic Acids
Original Article

miR-17-3p Downregulates Mitochondrial Antioxidant Enzymes and Enhances the Radiosensitivity of Prostate Cancer Cells

Zhi Xu,[1,2,5] Yanyan Zhang,[2,5] Jiaji Ding,[2] Weizi Hu,[2] Chunli Tan,[2] Mei Wang,[3] Jinhai Tang,[1,3] and Yong Xu[1,2,4]

[1]The Forth Clinical School of Nanjing Medical University, 140 Hanzhong Road, Nanjing 210029, China; [2]Jiangsu Cancer Hospital & Jiangsu Institute of Cancer Research & Nanjing Medical University Affiliated Cancer Hospital, 42 Baiziting, Nanjing 210009, China; [3]Department of General Surgery, First Affiliated Hospital with Nanjing Medical University, 300 Guangzhou Road, Nanjing 210029, China; [4]Jiangsu Key Lab of Cancer Biomarkers, Prevention and Treatment, Nanjing Medical University, 101 Longmian Avenue, Nanjing 211166, China

Radioresistance remains to be a major obstacle in the management of patients with advanced prostate cancer (PCa). We have identified a mature miR-17-3p processed from the 3′ arm of precursor miR-17, which appeared to be able to inhibit three major antioxidant enzymes located in mitochondria, i.e., manganese superoxide dismutase (MnSOD), glutathione peroxidase 2 (Gpx2), and thioredoxin reductase 2 (TrxR2). Here we show that upregulation of miR-17-3p remarkably sensitized PCa cells to ionizing radiation (IR). Reductions of the three antioxidants led to increasing cellular reactive oxygen species (ROS) accumulation as well as declining mitochondrial respiration. The miR-17-3p-mediated dysfunction of mitochondrial antioxidants apparently sensitizing IR therapy was manifested *in vitro* and *in vivo*. Substantially, the miR-17-3p effect on suppression of the antioxidants can be efficiently eliminated or attenuated by transfecting with either an miR-17-3p inhibitor or each of the related antioxidant cDNA expression constructs. Overall, in addition to the insights into the functional assessments for the duplex of miR-17-5p and miR-17-3p, the present study highlights the rigorous evidence that demonstrated suppression of multiple mitochondrial antioxidants by a single microRNA (miRNA), thereby providing a promising approach to improve radiotherapy for advanced PCa by targeting mitochondrial function.

INTRODUCTION

Globally, prostate cancer (PCa) is the most common malignant tumor and a major cause of cancer death in men. Owing to the improved early diagnosis and advanced therapeutics, the current death rate of PCa patients has been decreased in the United States. However, PCa morbidity and motility have been steadily increasing in East Asia.[1–3] Although radiotherapy is a main treatment opinion for localized PCa,[4] its therapeutic efficiency is eventually decreased due to most patients developing more aggressive forms of PCa that resist radiation. Accordingly, increasing the radiation dose may improve the therapeutic outcome, but it also increases the risk of damages to normal tissues or even leads to developing the second cancers in other organs, such as bladder, colorectal, and rectum.[5] Thus, PCa intrinsic radiosensitivity-mediated differences in susceptibility to radiotherapy largely affects clinical outcomes, including tumor-localized control and disease-free survival.[6]

Initiation of radioresistance remains to be fully elucidated. It is mainly caused by the activation of intrinsic resistant mechanisms in tumor cells like DNA repair pathways and/or the extrinsic intermediaries of therapeutic resistance through non-malignant cells, such as tumor stroma.[7] Virtually, radiation-induced reactive oxygen species (ROS) production beyond the cellular defense mechanisms could promote harmful oxidation and peroxidation chain reactions that damage nucleic acids, proteins, and lipids.[8] In this regard, DNA has been demonstrated to be the major target of radiation, and DNA double-strand breaks can be caused directly by irradiation energy or indirectly by ROS generated from water dissociation, including superoxide radical ($O_2^{\cdot -}$), hydroxyl radical ($^{\cdot}OH$), and hydrogen peroxide (H_2O_2), as well as other downstream oxidative products.[9] Indeed, there were two-thirds of radiation-mediated DNA damaged by indirect effects from ROS.[10,11] Nonetheless, tumor cells can adaptively synthesize more antioxidants to protect themselves against ROS.[12] In particular, the activation of primary antioxidant enzymes located in mitochondria has been shown to be essential for detoxification against radiation-generated ROS.[13] Consequently, the radiosensitivity of cancer cells can be enhanced by targeting cellular antioxidant defense systems.[14]

MicroRNAs (miRNAs), non-coding RNAs with a length of 18–25 bp, can suppress protein translation via binding to the 3′ UTR of target

Received 8 December 2017; accepted 15 August 2018;
https://doi.org/10.1016/j.omtn.2018.08.009.

[5]These authors contributed equally to this work.

Correspondence: Yong Xu, PhD, Jiangsu Cancer Hospital, Jiangsu Institute of Cancer Research, Nanjing Medical University Affiliated Cancer Hospital, 42 Baiziting, Nanjing 210009, China.
E-mail: yxu4696@njmu.edu.cn
Correspondence: Jinhai Tang, MD, Department of General Surgery, First Affiliated Hospital with Nanjing Medical University, 300 Guangzhou Road, Nanjing 210029, China.
E-mail: tangjh@njmu.edu.cn

mRNAs. The miRNA-mediated gene post-transcriptional regulation is involved in various aspects of physiogenesis and pathogenesis.[15,16] Numerous studies have demonstrated that miR-17-92 functions as oncogenic miRNA mainly through activating Akt- and ERK1/2-signaling pathways by downregulation of apoptotic protein BIM and tumor suppressor PTEN. Consistently, inhibition of the Akt-signaling pathway using antisense of miR-17-92 resulted in decreasing proliferation and chemoresistance of PCa cells.[17–19] Nevertheless, we previously identified miR-17-3p, processed from the 3′ arm of precursor miR-17, is able to suppress three mitochondrial antioxidant enzymes, manganese superoxide dismutase (MnSOD), glutathione peroxidase 2 (Gpx2), and thioredoxin reductase 2 (TrxR2).[20] They are major components of the primary antioxidant enzymes located in mitochondria to work in concert for efficiently removing ROS generated during mitochondrial respiration.[21] Coincidently, radioresistance of cancer cells is mainly mediated by increasing their antioxidants in response to high levels of ROS.[8,14,22,23] Therefore, the present study aims to examine whether miR-17-3p sensitizes aggressive PCa cells to ionizing radiation (IR) by inhibition of the three mitochondrial antioxidant enzymes. Our results demonstrated that upregulation of miR-17-3p in PCa cells remarkably inhibits mitochondrial antioxidant capacity and significantly increases the cell sensitivity to IR, suggesting that miR-17-3p may serve as a useful radiosensitizer for improving radiotherapy to treat advanced PCa.

RESULTS

miR-17-3p Enhances the Radiosensitivity of PC-3 Cells

Previously, we found that miR-17-3p is able to simultaneously suppress three major mitochondrial enzymes (MnSOD, Gpx2, and TrxR2) through specifically binding to the 3′ UTR of the genes (see also Figure S1). Upregulation of miR-17-3p resulted in suppression of PCa tumorigenicity.[20] Thus, we suspected that miR-17-3p may contribute to enhancing radiosensitivity of PCa cells due to its capacity to inhibit the cellular antioxidant defense system. To determine the potential effect of miR-17-3p on radiosensitization of androgen-independent aggressive PCa cells, we established a Tet-on inducible miR-17-3p expression PC-3 cell model and further confirmed by the determination of red fluorescent protein (RFP) tag expression (see also Figure S2A). The expression levels of miR-17-3p in the cells in response to the inducing reagent doxycycline (Dox) were quantified by qRT-PCR (see also Figure S2B). In addition, to confirm the effect of miR-17-3p in androgen receptor (AR)-positive PCa cells, an miR-17-3p or a scramble control was transfected into 22Rv1 cells and screened by green fluorescence (see also Figure S2C). The increased miR-17-3p expression was further confirmed by qRT-PCR (see also Figure S2D). Consequently, the reduced levels of three antioxidant proteins and the related enzyme activities in PC-3 and 22Rv1 cells were determined (see also Figures S3A–S3F).

It has been shown that cellular antioxidant ability is closely correlated to cell radioresistance.[14] To examine the radiosensitization effect of miR-17-3p, the miR-17-3p-expressing cells were irradiated. Cytotoxicity and the apoptotic rate were analyzed by 3-(4,5-dimethylthiazol-2yl)-2,5 diphenyltetrazolium bromide (MTT), colony formation, and flow cytometry, respectively. The results showed that the cell viability was significantly reduced in the miR-17-3p-expressing cells after exposure to IR (Figures 1A and 1C). Consistently, upregulation of miR-17-3p significantly increased the apoptotic rates following IR treatment (Figures 1B and 1D). Furthermore, clonogenic assays for the determination of cell survival rates were performed to confirm the cytotoxic effect of miR-17-3p on the enhancement of radiosensitivity of PCa cells. As shown in Figures 1E and 1F, the upregulation of miR-17-3p significantly increased IR-induced cell death.

In addition, we examined whether suppression of miR-17-3p in PCa cells could hyposensitize IR treatment. Transient transfection of the miR-17-3p inhibitor in PC-3 cells resulted in more than 2-fold decreases in miR-17-3p levels compared to a scramble control. Importantly, the application of miR-17-3p inhibitor can efficiently abrogate Dox-induced miR-17-3p in PC-3 cells (Figure 2A). Consistently, the results from cytotoxic analyses using the multiple methods as described above consistently showed that the suppression of miR-17-3p induction can reduce the apoptotic rates and rescue cells from IR-mediated cell death (Figures 2B–2F). Taken together, these results suggest that the expression levels of miR-17-3p are correlated to the radiosensitivity of PCa cells.

miR-17-3p Increases ROS Production and Decreases Mitochondrial Respiration

To determine the effect of miR-17-3p on IR-inducible intracellular ROS, the total cellular ROS was monitored using a dichlorofluorescein (DCF) assay. The levels of fluorescence-labeled ROS were significantly higher in IR-treated cells compared to the untreated group (Figures 3A and 3B), indicating that IR induces cell death partially through increasing the cellular ROS levels. Additionally, upregulation of miR-17-3p further increased the ROS levels. Thus, the elevated miR-17-3p expression presumably affects mitochondrial function due to its negative regulation of mitochondrial antioxidant enzymes. Furthermore, the high levels of ROS induced by IR were significantly decreased by N-acetyl-L-cysteine (NAC), a ROS inhibitor (Figures 3A and 3B). Consistently, NAC was able to rescue IR-induced cell death to a certain extent in PC-3 cells (Figures 3C and 3D), verifying that IR induces cell death partially through increasing the cellular ROS.

To assess the effect of miR-17-3p on mitochondrial respiration, after treatment, the mitochondrial oxygen consumption rates (OCRs) were quantified using a Seahorse Metabolic Analyzer Assay. IR appeared to increase all phases of mitochondrial respiration, while miR-17-3p showed itself to be negative for mitochondrial respiration; in particular, miR-17-3p attenuated IR-induced mitochondrial OCRs (Figures 3E and 3F). IR-generated ROS supposedly adaptively induces the expression of antioxidant enzymes to protect the cells. Conversely, miR-17-3p can suppress IR-induced antioxidant response, leading to increased ROS levels for cell death. These results suggest that miR-17-3p negatively regulates mitochondrial respiration through the inhibition of mitochondrial antioxidant enzymes.

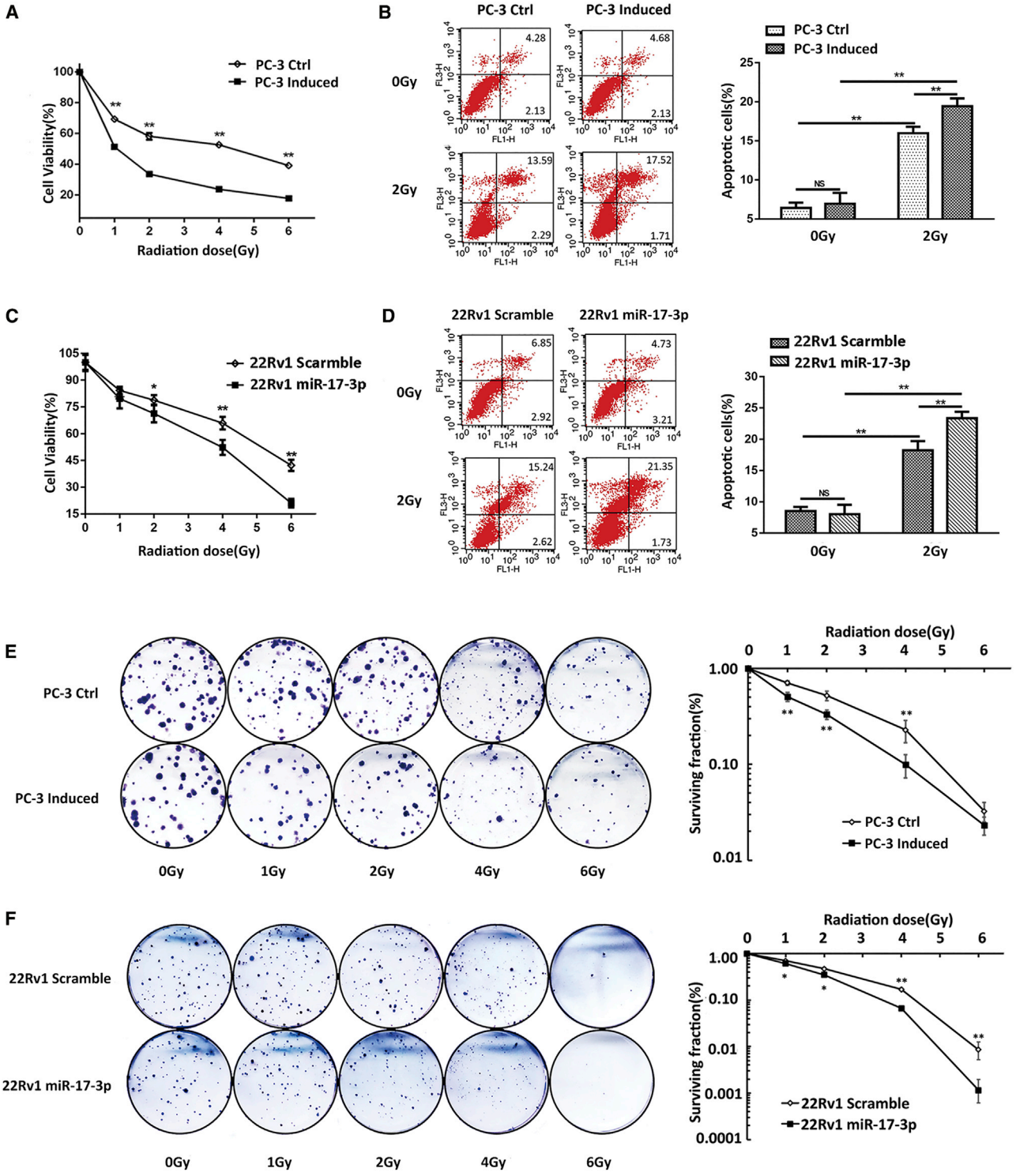

Figure 1. The Effect of miR-17-3p on the Radiosensitivity of PCa Cells

miR-17-3p was expressed in PC-3 cells based on a Tet-on regulation system, and the cells were treated with different doses of IR as indicated. (A) The cell viability was analyzed using an MTT assay, and (B) the apoptotic rate was quantified by flow cytometry. miR-17-3p was transfected into 22Rv1 cells. (C) The cell viability and (D) apoptotic rate were quantified. (E) PC-3 cell and (F) 22Rv1 surviving cell fractions were determined by colony formation. Values are presented as the mean ± SD ($n \geq 3$). NS, not significant. *$p < 0.05$ and **$p < 0.01$ present the significances between two groups as indicated.

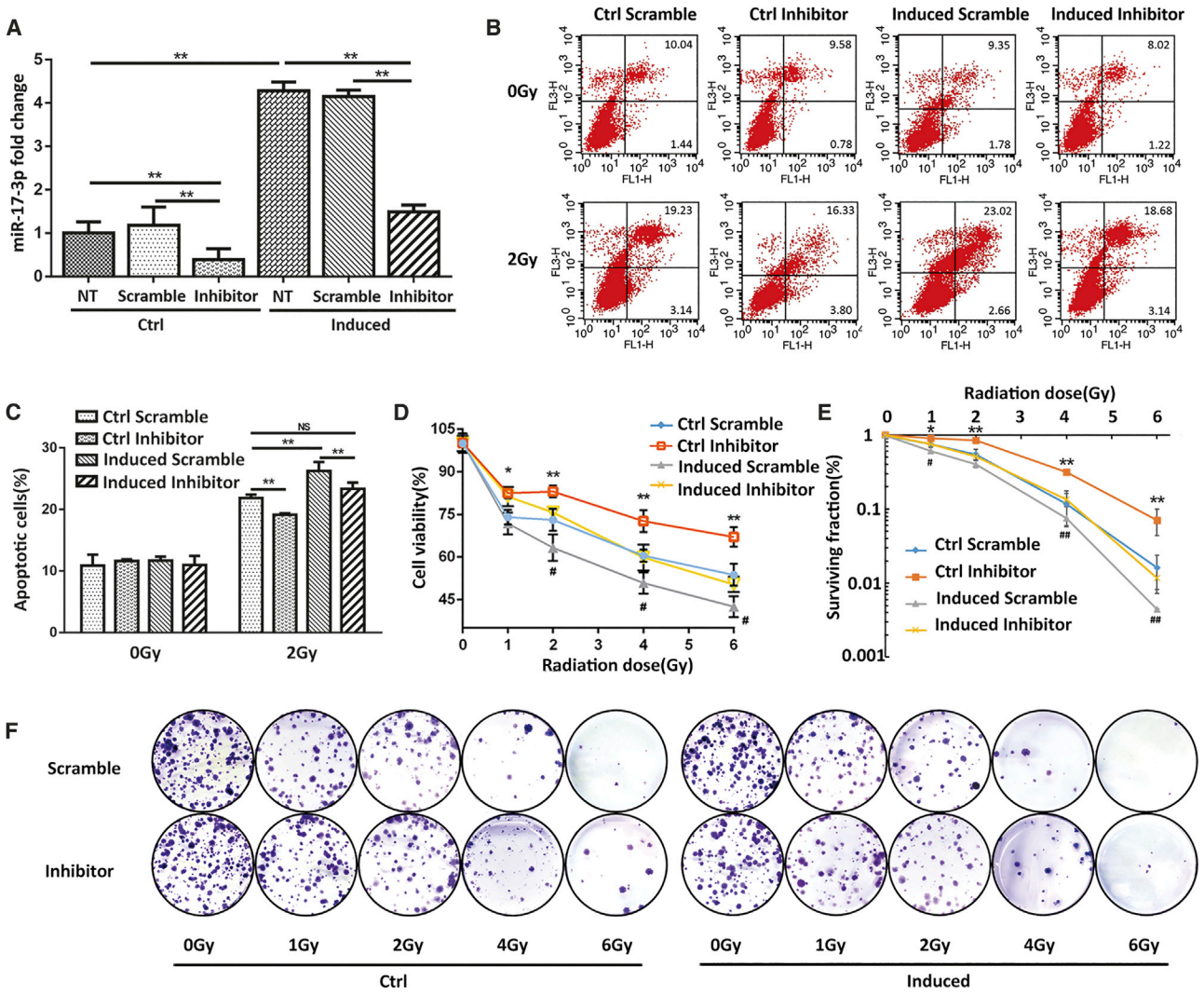

Figure 2. Reversal of the Radiosensitivity of PC-3 Cells by Transfection of miR-17-3p Inhibitor

(A) An miR-17-3p inhibitor or a scramble control was transiently transfected into Dox-induced PC-3 cells. NT indicates no oligo-transfected control. The levels of miR-17-3p were quantified by qRT-PCR. (B) The transfected cells were treated with 2-Gy IR, apoptotic cells were analyzed by flow cytometry, and (C) the apoptotic rates were calculated. (D–F) The transfected cells were treated with different doses of IR as indicated, and the cell viability and surviving fraction were determined by MTT (D) and colony formation (E and F), respectively. Values are presented as the mean ± SD ($n \geq 3$). NS, not significant. $^{*}p < 0.05/^{\#}p < 0.05$ and $^{**}p < 0.01/^{\#\#}p < 0.01$ present the significances between two groups as indicated.

miR-17-3p Enhances the Radiosensitivity of PC-3 Cells by Dysfunction of the Three Mitochondrial Antioxidant Enzymes

MnSOD, Gpx2, and TrxR2, the major components of the primary antioxidant system, functionally collaborate to efficiently remove ROS generated in mitochondria. It is well known that the conventional radiotherapy or chemotherapy can adaptively induce the antioxidant enzymes, leading to tumor therapeutic resistance. Consistently, downregulation of the antioxidant enzymes could sensitize tumor cells to treatment.[14] To determine whether miR-17-3p alters the radiosensitivity of PCa cells due to downregulation of mitochondrial antioxidants, the levels of MnSOD, Gpx2, and TrxR2 in PC-3 cells were quantified by qRT-PCR and western blots. The expression of antioxidant enzymes was significantly increased in IR-treated cells compared to untreated controls, while the ectopic expression of miR-17-3p further eliminated the IR effects on induction of antioxidants (Figures 4A and 4B). In addition, the activities of MnSOD, Gpx, and TrxR were also measured to confirm the effects of miR-17-3p on inhibition of the antioxidant enzymes (Figure 4C). In addition, the mitochondrial fraction was prepared to quantify the three antioxidants and their activities in mitochondria. Consistent with the results from the whole-cell extracts, the mitochondrial levels of the three antioxidant proteins

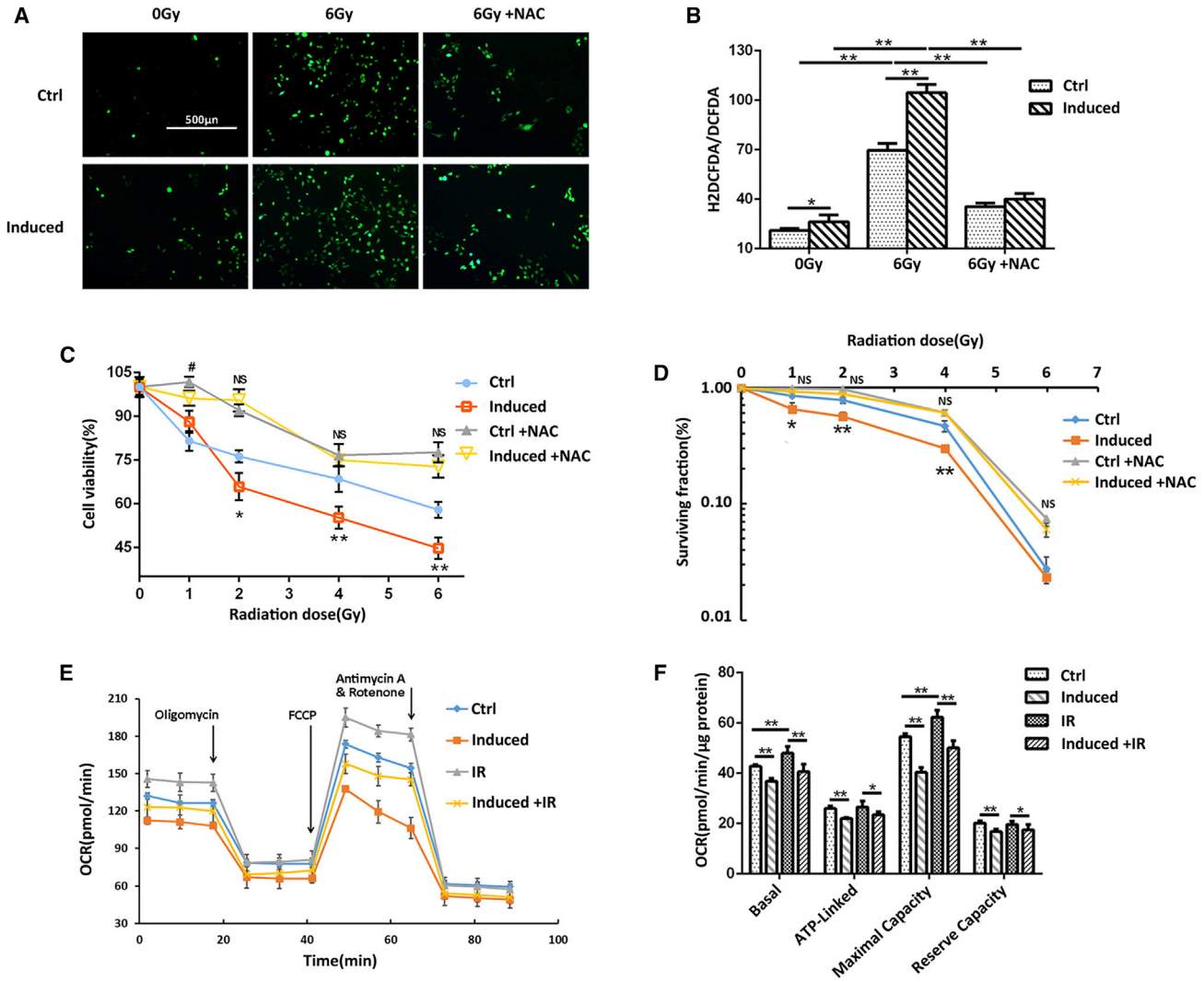

Figure 3. Quantification of ROS and Mitochondrial OCR in miR-17-3p-Expressing PC-3 Cells

(A) After treatment, the levels of cellular ROS were determined using a total cellular ROS detection kit. ROS inhibitor NAC was included to eliminate the IR-induced ROS. (B) The levels of ROS were calculated. The cells were treated with or without NAC followed by IR treatment as indicated. (C) The cell viability was quantified by MTT, and (D) the cell surviving fraction was determined by MTT and colony formation. (E) Mitochondrial OCR in the treated cells was measured using a Seahorse XF-96 analyzer. Supplemental reagents, including oligomycin, FCCP, and antimycin or rotenone, were automatically injected into the analyzing plates to determine the OCR of basal, ATP-linked, maximum, and background image, respectively. (F) The relative OCR was calculated, and the OCR reverse capacity, an important mitochondrial respiration index, was determined by the maximal OCR subtracted from the basal OCR. Values are presented as the mean ± SD ($n \geq 3$) and statistical significances between two groups are as described in Figure 2.

and relating enzymatic activities were induced by IR, but the IR effect was invalidated by miR-17-3p (Figures 4D and 4E). Furthermore, the effects of miR-17-3p on antioxidants and radiosensitivity were verified in 22Rv1 cells. Consistently, the expression levels and enzymatic activities of the three antioxidants were induced by IR treatment but eventually eliminated by overexpression of miR-17-3p (see also Figures S4A and S4B). These results suggest that miR-17-3p enhanced PCa cells to IR, mainly through abrogating IR-mediated induction of antioxidant enzymes.

miR-17-3p Inhibitor Sustains the Radioresistance of PC-3 Cells by Counteracting the miR-17-3p Effect

To further verify the mechanism by which miR-17-3p enhances the radiosensitivity of PC-3 cells, an miR-17-3p inhibitor was transiently transfected in the miR-17-3p-expressing PC-3 cells to determine its potential reversal effect on radiosensitization in the cells. As expected, the levels of cellular ROS were reduced by eliminating the effect of miR-17-3p (Figure 5A). Consistently, the cells with high levels of miR-17-3p led to suppression of the three antioxidant enzymes, but

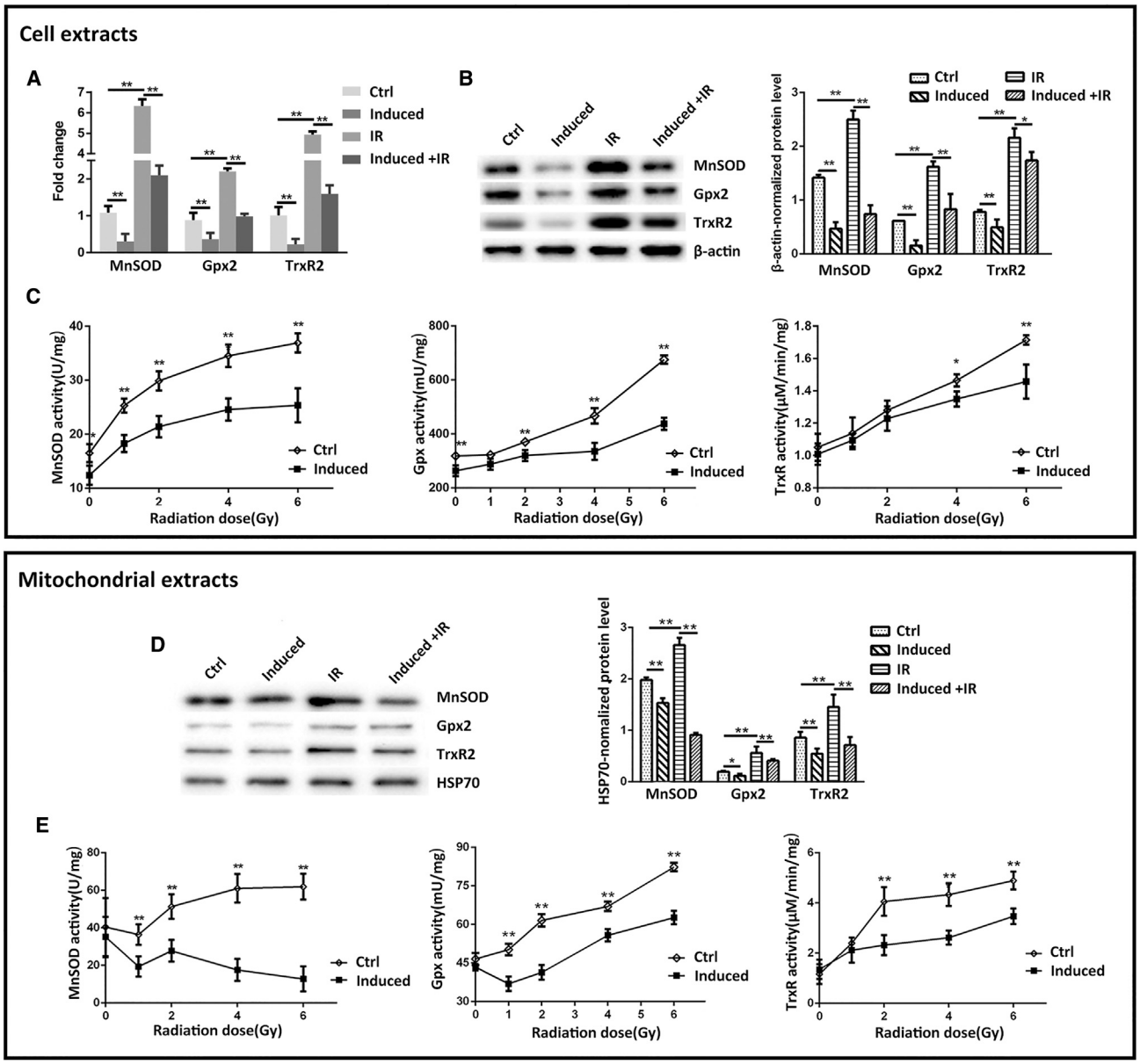

Figure 4. miR-17-3p-Mediated Suppression of IR-Induced Three Mitochondrial Antioxidants

(A) miR-17-3p was induced in PC-3 cells and then treated with 6-Gy IR. The mRNA levels of MnSOD, Gpx2, and TrxR2 were quantified by qRT-PCR and then normalized by β-actin mRNA. (B) The protein levels of the three antioxidant enzymes were determined by western blots with β-actin normalization. (C) The cells were treated with different doses of IR as indicated, and the activities of the three antioxidant enzymes were measured. Mitochondria were isolated from the treated cells, and (D) the three antioxidant proteins and (E) their enzymatic activities were quantified corresponding to (B) and (C). Values are presented as the mean ± SD ($n \geq 3$), and statistical significances between two groups are as described in Figure 1.

the effects were efficiently eliminated by applying the miR-17-3p inhibitor (Figure 5B). Furthermore, qRT-PCR and enzyme activity assay were performed to confirm that the transfected miR-17-3p inhibitor was able to neutralize miR-17-3p-mediated suppression of antioxidant enzymes (Figures 5C and 5D). These results further verified that the effect of miR-17-3p on radiosensitization is mediated by suppression of antioxidant enzymes in mitochondria.

Ectopic Expression of the Three Antioxidant Proteins Reverses the miR-17-3p-Enhanced Cell Death

To confirm whether the miR-17-3p-mediated radiosensitization is mainly through targeting MnSOD, Gpx2, and TrxR2, a cDNA construct for expressing each of the three antioxidant genes with a lack of the 3′ UTR was transiently transfected in the miR-17-3p-expressing PC-3 cells. The increased levels of mRNA and

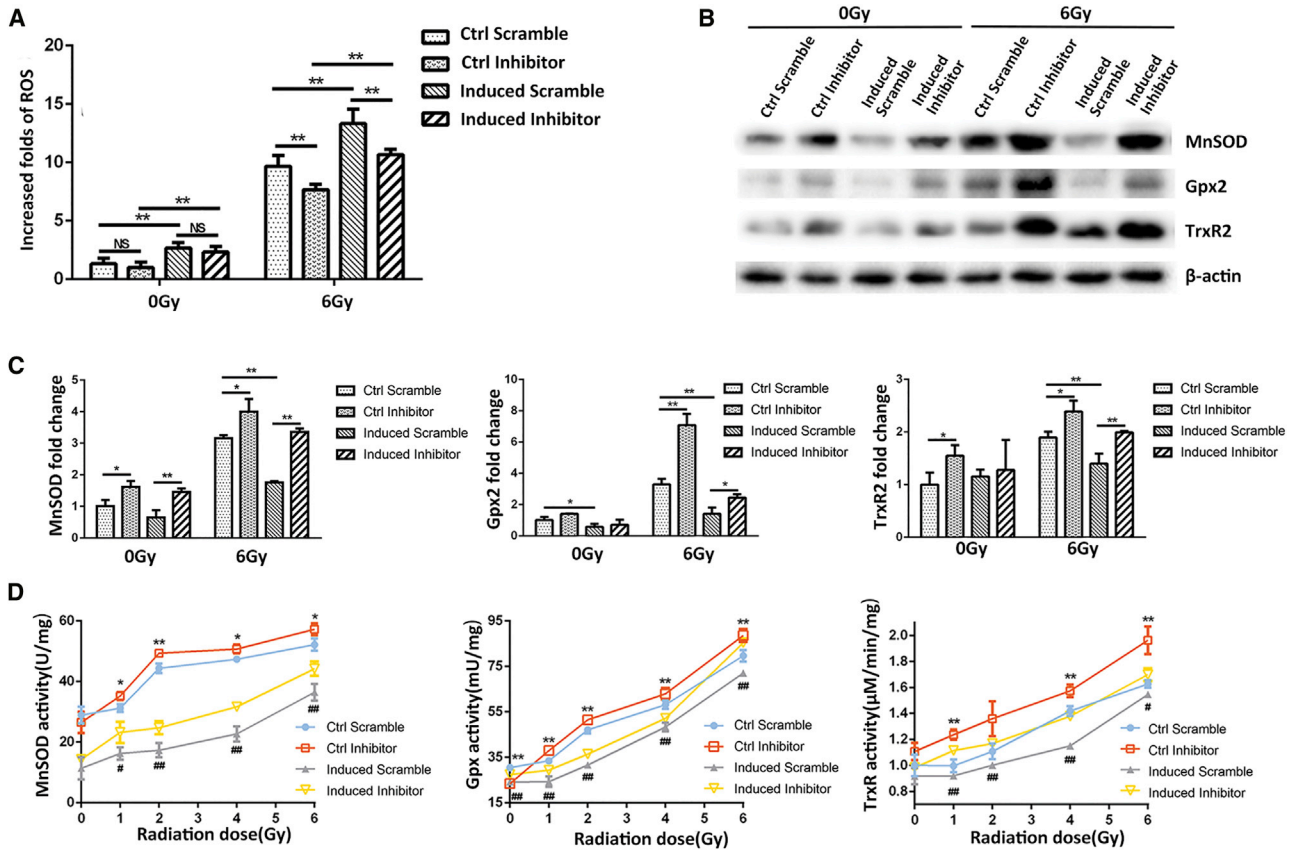

Figure 5. Reveal of the Reduction of Antioxidants by Transfection of miR-17-3p Inhibitor

(A) The miR-17-3p-induced cells were transiently transfected with miR-17-3p inhibitor prior to 6-Gy IR treatment. The levels of cellular ROS were quantified as described in Figure 3. (B) The related antioxidant proteins were determined by western blots with β-actin as a loading control. (C) The mRNA levels of the related antioxidant enzymes were quantified using qRT-PCR. (D) After treating with different doses of IR, the activities of the enzymes were measured as described in Figure 4. Values are presented as the mean ± SD ($n \geq 3$), and statistical significances between two groups are as described in Figure 2.

protein of each transfected cDNA were confirmed by qRT-PCR and western blots (Figures 6A and 6B). Correspondingly, the overexpression of each antioxidant gene resulted in decreasing ROS production in the cells, indicating that ectopic expression of the individual antioxidant gene can reduce miR-17-3p-enhanced high levels of ROS (Figure 6C). Subsequently, the reduced cytotoxicity was confirmed by MTT assay, and the rescued cell survival was determined by clonogenic assay (Figures 6D and 6E). These results indicated that increasing the individual antioxidant protein is able to, at least in part, reduce the cell death by decreasing ROS levels, supporting the finding that miR-17-3p enhances radiosensitization in PC-3 cells by targeting mitochondrial antioxidant enzymes.

Radiosensitization Effect of miR-17-3p Is Validated in Nude Mice

We established tumor-bearing male nude mice by subcutaneously injecting PC-3 cells with inducible upregulation of miR-17-3p. When the tumor reached 500 mm^3, the mice were divided into four groups as described above. During the xenograft tumor growth, there was no significant difference in tumor volumes among the 4 groups in the first 10 days. After giving different treatments at day 10, IR appeared to significantly inhibit tumor growth compared to the untreated groups. Importantly, the induction of miR-17-3p expression could further enhance radiotherapeutic efficacy (Figure 7A). Consistent with the tumor growth rates, tumor volume changes from day 10 to day 22 when tumors in the control group reached a maximal volume of 2,000 mm^3, the increased tumor volumes were apparently low in the treated groups as compared to the control group, particularly in the group of Dox-induced + IR (Figure 7B). The mice were executed and tumor tissues were excised to extract proteins when tumors reached the maximal volume. Consistent with the results from *in vitro* experiments, although IR highly induced the expression of the antioxidant proteins and their enzymatic activities, the upregulation of miR-17-3p could efficiently remove the effect of IR in the regulation of antioxidants (Figures 7C and 7D). Altogether, the present study demonstrates convincing evidence of the improved radiotherapy for advanced PCa by targeting mitochondrial antioxidants.

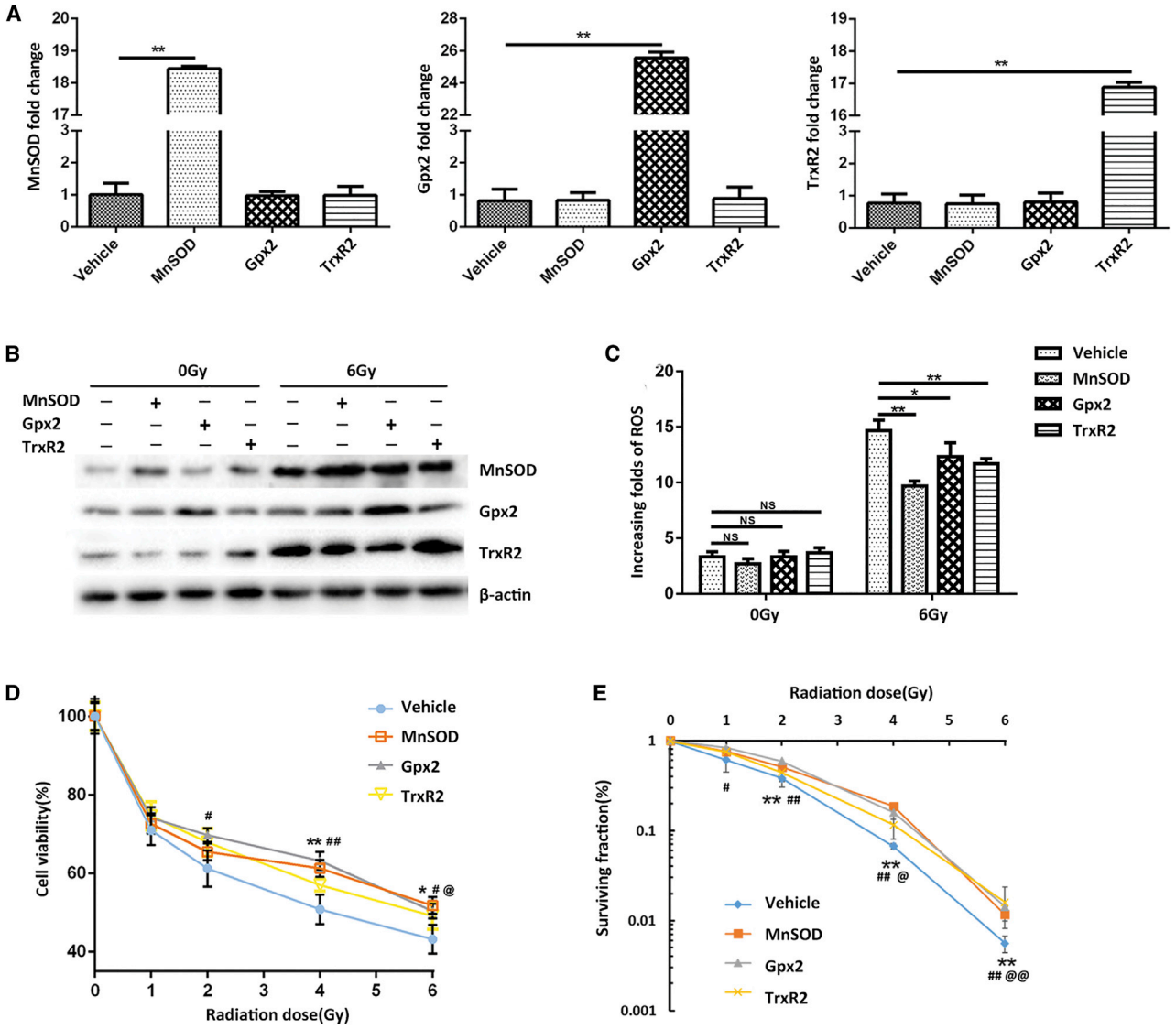

Figure 6. Diminishment of the miR-17-3p Effect by Ectopic Expression of Antioxidant Proteins

(A) The miR-17-3p-expressing PC-3 cells were transiently transfected with a cDNA construct of each antioxidant protein lacking the 3′ UTR. The mRNA levels of the antioxidants were quantified by qRT-PCR. (B) After transfection, the cells were treated with 6-Gy IR, and the protein levels of the antioxidants were determined by western blots. (C) The levels of cellular ROS in the treated cells were measured. (D) The transfected cells were treated with different doses of IR as indicated, and the cell viability was analyzed by MTT assay. (E) The cell surviving fraction was determined by colony formation. Values are presented as the mean ± SD ($n \geq 5$). In addition to $^{*}p < 0.05/^{\#}p < 0.05$ and $^{**}p < 0.01/^{\#\#}p < 0.01$, $^{@}p < 0.05$ and $^{@@}p < 0.01$ present the significances between two groups as described in Figure 2.

DISCUSSION

According to the recent statement issued by the American Cancer Society, PCa is estimated to account for approximately one in five new diagnoses of cancer in men in 2017.[24] Although the 5-year survival rate for PCa has increased in the United States, the death rate of PCa has been rising in some Asian and European countries, such as Korea, China, and Russia.[1] Radiotherapy has been extensively used as a curative treatment for localized PCa. It has been noted that escalating radiation doses to the range of 70–80 Gy essentially improves 5-year biochemical-free survival rate.[4] However, the clinical data also demonstrated that up to 50% of PCa patients undergo radioresistance within 5 years, indicating that intrinsic or acquired radioresistance has occurred during radiotherapy.[25] Thus, the discovery of novel radiosensitizers is urgently needed to enhance radiotherapeutic efficiency for the control of advanced PCa.[26] Numerous studies have identified various agents that were capable of sensitizing cancer cells to radiation. Unfortunately, most of the clinical trials have failed to present the promising results because of either their low efficacies or unexpected side effects.[7,27] Therefore, it still remains a big challenge to constantly discover

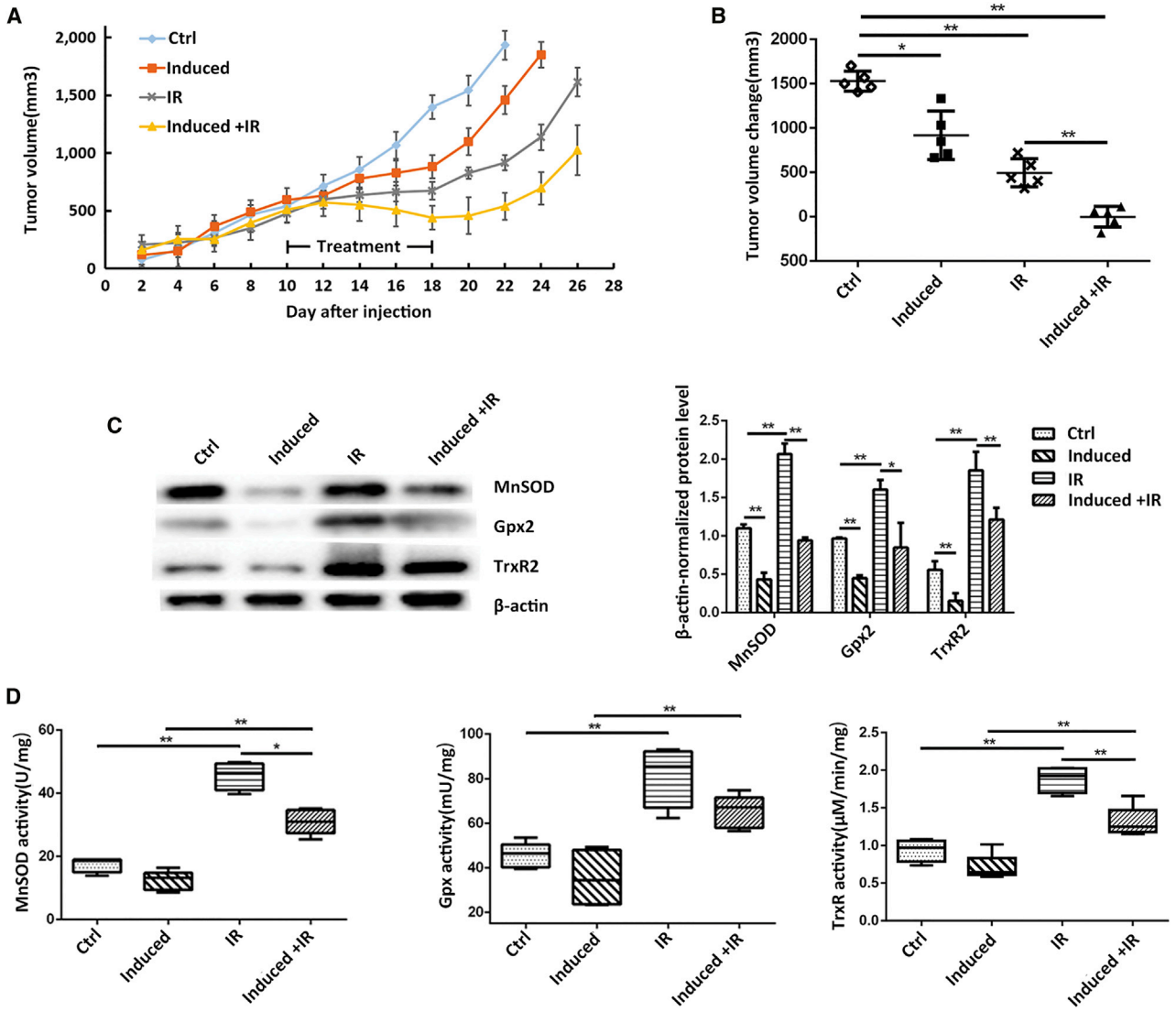

Figure 7. Validation of the miR-17-3p Radiosensitization Effect *In Vivo*

(A) Male nude mice were implanted with PC-3 cells and allowed tumor growing to reach 500 mm^3; the expression of miR-17-3p was induced by drinking Dox-containing water, and the tumors were treated with 5× 3-Gy IR as indicated. The tumor growths in the indicated groups were routinely measured. (B) Tumor volume changes in the different groups were calculated. (C) The levels of MnSOD, Gpx2, and TrxR2 in tumor tissues were determined by western blots with β-actin normalization. (D) The activities of the three antioxidant enzymes in the tumor tissues were measured. Values are presented as the mean ± SD ($n \geq 6$). Statistical significances between two groups are as described in Figure 1.

clinically useful radiosensitizers for the improvement of traditional radiotherapy.

It is well known that the principle of radiotherapy for killing cancer cells is mainly caused by ROS-mediated DNA damages.[9,28] Since the high doses of radiation are considered to provide more efficient outcomes for controlling aggressive tumor subtypes, the maximally tolerated radiation doses have already been tested to treat advanced PCa. However, since radiation-induced massive ROS exerts significant harmful effects on the structure of macromolecules, the widespread use of high-dose radiation imperatively increases the incidences of radiation-related genitourinary injury. Nonetheless, under the increased oxidative stress, the antioxidant defense systems in tumor cells are adaptively activated for cleavage of ROS. The scavengers of ROS, such as MnSOD, Gpx2, and TrxR2, have been proven to play pivotal roles for the detoxification of excessive ROS.[11,29] We and others have demonstrated that MnSOD is highly upregulated in a rapid response to radiation-generated ROS in PCa cells, suggesting that the activation of MnSOD is a major contributor to the radioresistance of PCa.[30,31] Consequently, multiple approaches have been

successfully used for improving PCa radiotherapy by suppressing MnSOD.[30,32]

MnSOD is a type of nuclear factor κB (NF-κB)-regulated protein and it is highly expressed in advanced PCa.[33] Radiotherapy quickly increases MnSOD expression, mainly through triggering the NF-κB-signaling pathway.[14] Thus, inhibition of the NF-κB-mediated transcriptional activation has attracted a lot of attention in the improvement of radiotherapy for aggressive tumors, including advanced PCa.[34,35] In addition, MnSOD-mediated radioresistance has been well established in breast cancer. The selected radioresistant MCF-7 cells showed hyperactive NF-κB signaling and a relating high level of MnSOD. Consequently, mitochondria-located SIRT3 is activated via Thr150/Ser159 phosphorylation by cyclin B1-CDK1, leading to increasing mitochondrial potential and ATP generation.[36] In search of more potential MnSOD suppressors, we surprisingly found that miR-17-3p is able to target three mitochondrial antioxidant enzymes. It is a very impressive finding because only suppression of MnSOD for reducing $O_2^{\cdot -}$ may not be efficient due to other downstream oxidative radicals, such as $^{\cdot}OH$ and H_2O_2, which may already be converted. Thus, the dysfunction of the three antioxidant enzymes in mitochondria may provide the best way to sufficiently enhance radiotherapeutic efficiency. The present study has validated the anticipated effect of miR-17-3p on radiosensitization *in vitro* and *in vivo*. With the declined antioxidant capacity, the cellular ROS levels were increased and the mitochondrial respiration rates were decreased accordingly. Our results suggest that miR-17-3p is a useful radiosensitizer for treating advanced PCa.

Numerous studies have demonstrated that the miR-17-92 cluster is highly expressed in various types of cancer, which contributes to the cancer progression and therapeutic resistances.[17,37] In particular, miR-17-5p has been shown to promote tumorigenesis of prostatic, pancreatic, and nasopharyngeal cancers.[18,38,39] Additionally, miR-17-5p also contributes to radioresistance in glioblastoma, gallbladder carcinoma, and esophageal adenocarcinoma cells.[40–42] However, the function of miR-17-3p in cancers remains elusive. We have previously demonstrated that mature miR-17-3p is able to suppress tumorigenicity of PCa cells via the inhibition of mitochondrial antioxidant enzymes, and recently its tumor suppressor function has also been reported in breast cancer.[43] In addition, mature miR-17-3p was also shown to negatively regulate pyruvate carboxylase-dependent cell proliferation in gallbladder cancer through regulating long noncoding RNA GCASPC.[41] Nevertheless, two studies from other groups reported that mature miR-17-5p and its passenger strand miR-17-3p enhance PCa growth due to repression of TIMP3 and also promote hepatocellular carcinoma by targeting multiple signal pathways, including PTEN.[19] It is speculated, therefore, that the effect of miR-17-3p may be subdued by miR-17-5p when they are mixed together. Indeed, we investigated the expression of miR-17-5p versus miR-17-3p in PCa, and the results showed that the ratio of miR-17-5p to miR-17-3p was largely increased in androgen-independent PCa cells compared to androgen-dependent PCa and normal prostate epithelial cells, indicating that the expression of miR-17-3p is silenced in advanced PCa.[20] Furthermore, under radiotherapeutic conditions, the expression of miR-17-3p was upregulated in irradiated human lymphoblast TK6 cells, and the level of miR-17-3p in glioblastoma cells was also shown to be relevant to radiosensitivity.[44,45] Overall, these results suggest that miR-17-3p may play a negative regulatory role in tumorigenicity and therapeutic resistance.

Notably, the function of miR-17-3p has been reported to be relevant to cellular redox homeostasis.[46] As targets of miR-17-3p, MnSOD, Gpx2, and TrxR2 were also confirmed by other groups.[47,48] Radiation is a potent inducer for ROS generation, thus it is a proposed strategy for sustaining radiotherapeutic efficiency to keep the high levels of ROS by the inactivation of antioxidant function. To reach the goal, miR-17-3p was tested in the present study for validating its potential function in consistently inhibiting the responsiveness of antioxidant enzymes under radiotherapeutic conditions. Our results verified that upregulation of miR-17-3p efficiently diminished IR-mediated antioxidant responses by simultaneously suppressing MnSOD, Gpx2, and TrxR2. Consequently, the cellular ROS level was increased and mitochondrial reparation was decreased by the dysfunction of antioxidants. In addition, to verify that the suppression of antioxidants plays a causal role in the miR-17-3p-mediated radiosensitization, MnSOD, Gpx2, and TrxR2 were individually tested to restore the radioresistance by ectopically expressing their cDNA in the miR-17-3p-expressing cells. The results confirmed that the ectopic expression of each protein could partially rescue the cell survival by diminishing the effect of miR-17-3p. Thus, we conclude that the miR-17-3p-mediated downregulation of the three antioxidant enzymes promotes IR-induced damages by the accumulation of ROS.

In summary, the present study demonstrates that the manipulation of miR-17-3p supposedly affects the cellular redox status due to its ability of targeting antioxidants. In this context, the inactivation of antioxidants by expressing miR-17-3p should increase ROS and enhance radiotherapeutic efficiency to treat aggressive tumors. Our results provide proof-of-concept evidence that the inhibition of mitochondrial function by targeting its antioxidant defense system contributes to radiosensitization in advanced PCa cells. According to the previous novel finding that miR-17-3p can suppress the three mitochondrial antioxidant enzymes, the subsequent application of miR-17-3p for enhancing PCa cells to radiation provides a hopeful therapeutic approach for improving radiotherapy for the treatment of advanced PCa.

MATERIALS AND METHODS

Cell Culture and Treatment

Human prostatic adenocarcinoma PC-3 and carcinoma 22Rv1 cell lines were purchased from American Type Culture Collection (ATCC, USA), and the cells were maintained in RPMI 1640 medium (Invitrogen, USA) with 10% fetal bovine serum (Gemini, USA) plus a mixture of penicillin-streptomycin (100 U/mL–100 μg/mL, Invitrogen, USA) at 37°C in a humidified 5% CO_2

atmosphere. A Tet-on inducible lentiviral miR-17-3p construct was stably transducted into PC-3 cells, and miR-17-3p expression was induced by treating the cells with 0.5 μg/mL Dox (Invitrogen, USA). For increasing the level of miR-17-3p in 22Rv1 cells, miR-17-3p (5′-ACUGCAGUGAAGGCACUUGUAG-3′) and negative control with scramble sequence (5′-UUCUCCGAACGUGUC ACGU-3′) were synthesized by Shanghai Gene Pharma, China, and then transfected into the cells using an oligofectamine reagent (Invitrogen, USA), following the manufacturer's instructions. To determine the effect of miR-17-3p on the sensitivity of PCa cells to IR, the cells were treated with IR at a range of 0–6 Gy using an X-ray machine (RAD Source RS2000 X-ray, USA).

ROS Quantification

A DCF assay was used to quantify the levels of intracellular ROS. The cells were pretreated with or without 10 mmol/L NAC (Beyotime Biotechnology, China) for 1 hr, followed by IR treatment. At 3 hr after treatment, the cells were labeled by both H2DCF-DA (2,7-Dichlorodi-hydrofluorescein diacetate, sensitive to oxidation; Sigma, USA) and DCF-DA (insensitive to oxidation, Sigma, USA) at a final concentration of 5 μM in culture medium at 37°C for 30 min. Fluorescent images of DCF in the cells were observed using a fluorescence microscope (Nikon Ti, Japan) and then quantified by λexcitation 495 nm and λemission 520 nm using a TECAN Infinite M200 fluorescence spectrometer (Tecan, Switzerland). The H2DCF-DA:DCF-DA ratio was used to optimize the controls of cell number, dry uptake, and ester cleavage.

Apoptosis Analysis

Flow cytometry was used to quantify apoptotic cells after IR treatment. 2×10^5cells were seeded in 60-mm dishes overnight and treated with IR. To confirm the effect of miR-17-3p on apoptosis, miR-17-3p-expressing PC-3 cells were transfected with an miR-17-3p inhibitor (5′-CUACAAGUGCCUUCACUGCAGU-3′) or a negative control with scramble sequence (5′-CAGUACUUUUGUGUA GUACAA-3′) prior to IR treatment. At 1 day after treatment, the cells were collected and washed three times with a cold PBS. The cells were then stained within a binding buffer containing 5 μM annexin V-fluorescein isothiocyanate (FITC) (BD Biosciences, USA) and 2.5 μM propidium iodide (PI; Dojindo Molecular Technologies, Japan) for 15 min at room temperature and dark condition. FITC fluorescence intensity in 10,000 cells was measured using a BD FACS Calibur flow cytometer (BD Biosciences, USA). The apoptotic rates were calculated by number of proapoptotic and apoptotic cells divided by the amount of total cells.

Cell Viability Detection

MTT assay was used to determine cell viability after IR treatment. Cells were seeded in 96-well plates at a density of 5×10^3 cells/well. After treatment, the cells were incubated with 1 mg/mL MTT solution for a 4-hr incubation. After removing the media, the formazan products were solubilized with 200 μL dimethyl sulfoxide. Cell viability was assessed by measuring absorbance at 562 nm using a Thermo microplate reader (Thermo Fisher Scientific, USA).

Clonogenic Assay

Colony survival was used to quantify the cell death after IR treatment. 100–500 cells were plated in 6-well plates overnight and then treated with IR (0, 1, 2, 4, and 6 Gy). The treated cells were cultured allowing colony formation. After washing with PBS twice, the colonies were stained with 1% crystal violet dye for 30 min to form visible cell clones. The cell surviving fractions were calculated based on the ratio of the number of colonies formed to the number of cells efficiently plated. The cell death was determined by three independent experiments and plotted as mean ± SD.

Quantification of Oxygen Consumption

Mitochondrial respiration was assessed by measurement of OCR using a Seahorse XF96 Analyzer (Seahorse Bioscience, USA). After treatment, the cells were transferred into a 96-well XF96 plate at a cell density of 5×10^3 cells/well and incubated overnight. Cartridge plates for metabolic stress injections were hydrated for 24 hr at 37°C without CO_2 in calibrant solution. At 1 hr prior to the assay, the cultural medium in the XF96 plate was replaced by a Seahorse assay medium. OCR was measured under the following four conditions: basal, 1 μM oligomycin, 0.3 μM carbonyl cyanide-4-phenylhydrazone (FCCP), and 0.5 μM rotenone + 0.5 μM antimycin A. OCR was normalized by the total protein concentration.

Mitochondria Isolation

The isolation of an enriched mitochondrial fraction from PCa cells was performed using a Mitochondrial Isolation Kit (Sigma, USA), according to the manufacturer's instruction. Briefly, the cells were collected and washed once with cold PBS, and 2×10^7 cells were lysed in 1 mL homogenization buffer by 25 strokes in a homogenizer. After being incubated on ice for 15 min, the homogenate was centrifuged at $600 \times g$ for 10 min at 4°C to precipitate the nuclei, and the resulting supernatant was further centrifuged at $11{,}000 \times g$ for 10 min at 4°C to precipitate the mitochondrial fraction.

RNA Isolation and qRT-PCR

Total RNA was isolated from the treated cells by Tirzol preparation. Reverse transcription was performed using a PrimeScript RT reagent kit (Takara Bio, Japan), according to the manufacturer's instructions. qPCR was performed using a SYBR Premix Ex Taq (Takara Bio, Japan) by a LightCycle System (Roche, USA). Sequences of the qPCR primers are listed in Table S1.

Western Blots

Cells or tumor tissues were harvested and total proteins were extracted using a radioimmunoprecipitation assay (RIPA) buffer with 1 mM phenylmethylsulfonyl fluoride. The extracted proteins (50–100 μg) were separated on a 10% SDS-PAGE and then transferred onto a polyvinylidene fluoride (PVDF) membrane. The membrane was blocked in 5% skim milk for 2 hr and then washed three times for 15 min using a TBST solution (Tris-buffered saline containing 0.05% Tween-20). Subsequently, the membranes were incubated overnight at 4°C with the primary antibodies against MnSOD (Cell Signaling Technology, USA), Gpx2 (Abcam, UK), TrxR2 (Abcam,

UK), and β-actin (Cell Signaling Technology, USA). After washing with TBST three times for 15 min, the membranes were incubated for 2 hr with a peroxidase-conjugated goat anti-mouse immunoglobulin G (IgG) (Santa Cruz Biotechnology, USA) or a goat anti-rabbit IgG (Santa Cruz Biotechnology, USA). The immunoblotting was visualized using an enhanced chemiluminescence detection system (Bio-Rad, USA). The intensities of blots were normalized by β-actin as a loading control and then analyzed using Image Lab software.

Measurement of Antioxidant Enzyme Activity

After treatment, cell and tissue extracts were used to measure the activities of antioxidant enzymes using the relating kits and reagents. The extracts were prepared using an ultrasonic cell disruption system and collected by centrifugation at 10,000 rpm for 15 min at 4°C. To measure enzyme activity, the extracts were further centrifuged at 12,000 rpm at 4°C for 10 min to completely remove debris. The supernatants were subjected to an SOD assay kit (Beyotime Biotechnology, China) for measuring MnSOD activity, according to the manufacturer's protocol. The kit contains a Cu/ZnSOD inhibitor and WST-8 (2-(2-methoxy-4-nitrophenyl)-3-(4-nitrophenyl)-5-(2,4-disulfophenyl)-2H-tetrazolium), which produced a highly water-soluble formazan dye that can be inhibited by SOD. The optical density (OD) values were measured at 450 nm using a microplate reader (BioTek synergy 2, USA), and MnSOD activity was calculated using a formula as described in the manufacturer's instructions. Gpx activity was measured using a Gpx assay kit (Beyotime Biotechnology, China),[49] which can measure the coupled oxidation of NADPH during glutathione reductase (GR) recycling of oxidized glutathione from Gpx-mediated reduction of t-butyl peroxide. During the assay, excess GR, glutathione, and NADPH were sequentially added according to the manufacturer's instruction. TrxR activity was measured using a fluorescence assay kit containing thioredoxin reductase (Cayman Chemical, USA), according to the manufacturer's protocol.[50] The extracts were added in a diluted assay buffer (0.2 mg/mL BSA in 50 mM Tris-Cl and 1 mM EDTA [pH 7.5]) containing NADPH in 96-well plates and incubated for 30 min at 37°C. After adding a fluorescent substrate, OD (emission at 545 nm, excitation at 520 nm) was measured using TECAN Infinite M200 (Tecan, Switzerland). The concentration of TrxR was calculated using the increased fluorescent intensities at the defined reaction times according to the standard curve.

Animals

Animal experiments were performed according to the Institutional Animal Care and Use approved by the Research Committee of Nanjing Medical University (IACUC-1601229). The 5-week-old male nude (BALB/c) mice (Beijing Vital River Lab Animal Technology, China) were used for mouse xenograft tumor experiments. 5×10^6 cells from the logarithmic growth phase were subcutaneously implanted into the left flanks of mice and allowed to form the xenograft tumors. After tumor volume reached 500 mm^3, the mice were randomly divided into four groups: saline control, Dox induced, saline + 5× 3-Gy IR, and Dox + 5× 3-Gy IR Induced. At 2 days before IR treatment, Dox was added into the mice's drinking water at the final concentration of 2 mg/L and replaced every other day to the end of experiments. IR treatments were given every other day for 5 times with 3 Gy/day. Tumor volumes were measured using digital calipers every other day and calculated using a standard formula ($V = 0.52 \times AB^2$, where A and B represent the diagonal tumor lengths). The mice were executed when tumor volume reached 2,000 mm^3 and tumor tissues were removed for the following experiments.

Statistical Analysis

Data are presented as the mean ± SD of at least three replicates. Significant differences between two groups were analyzed by unpaired Student's t test. One-way ANOVA followed by Dunnett's or Bonferroni multiple comparison test was applied for multiple-group experiments using Prism (GraphPad, USA). Statistical significance was accepted at $p < 0.05$.

SUPPLEMENTAL INFORMATION

Supplemental Information includes four figures and one table and can be found with this article online at https://doi.org/10.1016/j.omtn.2018.08.009.

AUTHOR CONTRIBUTIONS

Z.X., Y.Z., and Y.X. designed the research. Z.X., Y.Z., J.D., W.H., C.T., and M.W. conducted the experiments. Z.X., Y.Z., and Y.X. analyzed and interpreted the data. Z.X. and Y.X. wrote the paper. J.T. and Y.X. supervised the research and provided administrative, technical, and material supports.

CONFLICTS OF INTEREST

The authors have no conflicts of interest.

ACKNOWLEDGMENTS

We thank Dr. Daret K. St. Clair, University of Kentucky Markey Cancer Center, for her kind suggestions and providing relating cell lines to accomplish this study. This research was supported by the National Program Project for Precision Medicine in National Research and Development Plan, China (2016YFC0905900 to Y.X. and J.T.), the National Natural Science Foundation of China Research Grants (81372199 and 81572742 to Y.X.), and the Natural Science Foundation of Jiangsu Province (BK20151579 to J.T.).

REFERENCES

1. Center, M.M., Jemal, A., Lortet-Tieulent, J., Ward, E., Ferlay, J., Brawley, O., and Bray, F. (2012). International variation in prostate cancer incidence and mortality rates. Eur. Urol. *61*, 1079–1092.

2. Torre, L.A., Bray, F., Siegel, R.L., Ferlay, J., Lortet-Tieulent, J., and Jemal, A. (2015). Global cancer statistics, 2012. CA Cancer J. Clin. *65*, 87–108.

3. Fitzmaurice, C., Allen, C., Barber, R.M., Barregard, L., Bhutta, Z.A., Brenner, H., Dicker, D.J., Chimed-Orchir, O., Dandona, R., Dandona, L., et al.; Global Burden of Disease Cancer Collaboration (2017). Global, Regional, and National Cancer Incidence, Mortality, Years of Life Lost, Years Lived With Disability, and Disability-Adjusted Life-years for 32 Cancer Groups, 1990 to 2015: A Systematic Analysis for the Global Burden of Disease Study. JAMA Oncol. *3*, 524–548.

4. Mottet, N., Bellmunt, J., Bolla, M., Briers, E., Cumberbatch, M.G., De Santis, M., Fossati, N., Gross, T., Henry, A.M., Joniau, S., et al. (2017). EAU-ESTRO-SIOG Guidelines on Prostate Cancer. Part 1: Screening, Diagnosis, and Local Treatment with Curative Intent. Eur. Urol. *71*, 618–629.
5. Wallis, C.J., Mahar, A.L., Choo, R., Herschorn, S., Kodama, R.T., Shah, P.S., Danjoux, C., Narod, S.A., and Nam, R.K. (2016). Second malignancies after radiotherapy for prostate cancer: systematic review and meta-analysis. BMJ *352*, i851.
6. Hanahan, D., and Weinberg, R.A. (2011). Hallmarks of cancer: the next generation. Cell *144*, 646–674.
7. Chang, L., Graham, P.H., Hao, J., Bucci, J., Cozzi, P.J., Kearsley, J.H., and Li, Y. (2014). Emerging roles of radioresistance in prostate cancer metastasis and radiation therapy. Cancer Metastasis Rev. *33*, 469–496.
8. Negre-Salvayre, A., Coatrieux, C., Ingueneau, C., and Salvayre, R. (2008). Advanced lipid peroxidation end products in oxidative damage to proteins. Potential role in diseases and therapeutic prospects for the inhibitors. Br. J. Pharmacol. *153*, 6–20.
9. Cadet, J., and Wagner, J.R. (2013). DNA base damage by reactive oxygen species, oxidizing agents, and UV radiation. Cold Spring Harb. Perspect. Biol. *5*, a012559.
10. Jayakumar, S., Kunwar, A., Sandur, S.K., Pandey, B.N., and Chaubey, R.C. (2014). Differential response of DU145 and PC3 prostate cancer cells to ionizing radiation: role of reactive oxygen species, GSH and Nrf2 in radiosensitivity. Biochim. Biophys. Acta *1840*, 485–494.
11. Holley, A.K., Miao, L., St Clair, D.K., and St Clair, W.H. (2014). Redox-modulated phenomena and radiation therapy: the central role of superoxide dismutases. Antioxid. Redox Signal. *20*, 1567–1589.
12. Wang, K., Zhang, T., Dong, Q., Nice, E.C., Huang, C., and Wei, Y. (2013). Redox homeostasis: the linchpin in stem cell self-renewal and differentiation. Cell Death Dis. *4*, e537.
13. Fridovich, I. (1978). The biology of oxygen radicals. Science *201*, 875–880.
14. Fisher, C.J., and Goswami, P.C. (2008). Mitochondria-targeted antioxidant enzyme activity regulates radioresistance in human pancreatic cancer cells. Cancer Biol. Ther. *7*, 1271–1279.
15. Fernandez-L, A., Northcott, P.A., Taylor, M.D., and Kenney, A.M. (2009). Normal and oncogenic roles for microRNAs in the developing brain. Cell Cycle *8*, 4049–4054.
16. Ni, J., Bucci, J., Chang, L., Malouf, D., Graham, P., and Li, Y. (2017). Targeting MicroRNAs in Prostate Cancer Radiotherapy. Theranostics *7*, 3243–3259.
17. Mendell, J.T. (2008). miRiad roles for the miR-17-92 cluster in development and disease. Cell *133*, 217–222.
18. Zhou, P., Ma, L., Zhou, J., Jiang, M., Rao, E., Zhao, Y., and Guo, F. (2016). miR-17-92 plays an oncogenic role and conveys chemo-resistance to cisplatin in human prostate cancer cells. Int. J. Oncol. *48*, 1737–1748.
19. Yang, X., Du, W.W., Li, H., Liu, F., Khorshidi, A., Rutnam, Z.J., and Yang, B.B. (2013). Both mature miR-17-5p and passenger strand miR-17-3p target TIMP3 and induce prostate tumor growth and invasion. Nucleic Acids Res. *41*, 9688–9704.
20. Xu, Y., Fang, F., Zhang, J., Josson, S., St Clair, W.H., and St Clair, D.K. (2010). miR-17* suppresses tumorigenicity of prostate cancer by inhibiting mitochondrial antioxidant enzymes. PLoS ONE *5*, e14356.
21. Lei, X.G., Zhu, J.H., Cheng, W.H., Bao, Y., Ho, Y.S., Reddi, A.R., Holmgren, A., and Arnér, E.S. (2016). Paradoxical Roles of Antioxidant Enzymes: Basic Mechanisms and Health Implications. Physiol. Rev. *96*, 307–364.
22. Liang, Y.W., Zheng, J., Li, X., Zheng, W., and Chen, T. (2014). Selenadiazole derivatives as potent thioredoxin reductase inhibitors that enhance the radiosensitivity of cancer cells. Eur. J. Med. Chem. *84*, 335–342.
23. Yang, W., Shen, Y., Wei, J., and Liu, F. (2015). MicroRNA-153/Nrf-2/GPx1 pathway regulates radiosensitivity and stemness of glioma stem cells via reactive oxygen species. Oncotarget *6*, 22006–22027.
24. Siegel, R.L., Miller, K.D., and Jemal, A. (2017). Cancer Statistics, 2017. CA Cancer J. Clin. *67*, 7–30.
25. Cooper, B.T., and Sanfilippo, N.J. (2015). Concurrent chemoradiation for high-risk prostate cancer. World J. Clin. Oncol. *6*, 35–42.
26. Rodier, F., and Campisi, J. (2011). Four faces of cellular senescence. J. Cell Biol. *192*, 547–556.
27. Alberti, C. (2014). Prostate cancer: radioresistance molecular target-related markers and foreseeable modalities of radiosensitization. Eur. Rev. Med. Pharmacol. Sci. *18*, 2275–2282.
28. Turesson, I., Carlsson, J., Brahme, A., Glimelius, B., Zackrisson, B., and Stenerlöw, B.; Swedish Cancer Society Investigation Group (2003). Biological response to radiation therapy. Acta Oncol. *42*, 92–106.
29. Valko, M., Rhodes, C.J., Moncol, J., Izakovic, M., and Mazur, M. (2006). Free radicals, metals and antioxidants in oxidative stress-induced cancer. Chem. Biol. Interact. *160*, 1–40.
30. Xu, Y., Fang, F., St Clair, D.K., Josson, S., Sompol, P., Spasojevic, I., and St Clair, W.H. (2007). Suppression of RelB-mediated manganese superoxide dismutase expression reveals a primary mechanism for radiosensitization effect of 1alpha,25-dihydroxyvitamin D(3) in prostate cancer cells. Mol. Cancer Ther. *6*, 2048–2056.
31. Hosseinimehr, S.J. (2015). The protective effects of trace elements against side effects induced by ionizing radiation. Radiat. Oncol. J. *33*, 66–74.
32. Eldridge, A., Fan, M., Woloschak, G., Grdina, D.J., Chromy, B.A., and Li, J.J. (2012). Manganese superoxide dismutase interacts with a large scale of cellular and mitochondrial proteins in low-dose radiation-induced adaptive radioprotection. Free Radic. Biol. Med. *53*, 1838–1847.
33. Holley, A.K., Xu, Y., St Clair, D.K., and St Clair, W.H. (2010). RelB regulates manganese superoxide dismutase gene and resistance to ionizing radiation of prostate cancer cells. Ann. N Y Acad. Sci. *1201*, 129–136.
34. Pordanjani, S.M., and Hosseinimehr, S.J. (2016). The Role of NF-kB Inhibitors in Cell Response to Radiation. Curr. Med. Chem. *23*, 3951–3963.
35. Mendonca, M.S., Turchan, W.T., Alpuche, M.E., Watson, C.N., Estabrook, N.C., Chin-Sinex, H., Shapiro, J.B., Imasuen-Williams, I.E., Rangel, G., Gilley, D.P., et al. (2017). DMAPT inhibits NF-κB activity and increases sensitivity of prostate cancer cells to X-rays in vitro and in tumor xenografts in vivo. Free Radic. Biol. Med. *112*, 318–326.
36. Liu, R., Fan, M., Candas, D., Qin, L., Zhang, X., Eldridge, A., Zou, J.X., Zhang, T., Juma, S., Jin, C., et al. (2015). CDK1-Mediated SIRT3 Activation Enhances Mitochondrial Function and Tumor Radioresistance. Mol. Cancer Ther. *14*, 2090–2102.
37. Weng, H., Huang, H., Dong, B., Zhao, P., Zhou, H., and Qu, L. (2014). Inhibition of miR-17 and miR-20a by oridonin triggers apoptosis and reverses chemoresistance by derepressing BIM-S. Cancer Res. *74*, 4409–4419.
38. Chen, C., Lu, Z., Yang, J., Hao, W., Qin, Y., Wang, H., Xie, C., and Xie, R. (2016). MiR-17-5p promotes cancer cell proliferation and tumorigenesis in nasopharyngeal carcinoma by targeting p21. Cancer Med. *5*, 3489–3499.
39. Quattrochi, B., Gulvady, A., Driscoll, D.R., Sano, M., Klimstra, D.S., Turner, C.E., and Lewis, B.C. (2017). MicroRNAs of the mir-17∼92 cluster regulate multiple aspects of pancreatic tumor development and progression. Oncotarget *8*, 35902–35918.
40. Comincini, S., Allavena, G., Palumbo, S., Morini, M., Durando, F., Angeletti, F., Pirtoli, L., and Miracco, C. (2013). microRNA-17 regulates the expression of ATG7 and modulates the autophagy process, improving the sensitivity to temozolomide and low-dose ionizing radiation treatments in human glioblastoma cells. Cancer Biol. Ther. *14*, 574–586.
41. Ma, M.Z., Zhang, Y., Weng, M.Z., Wang, S.H., Hu, Y., Hou, Z.Y., Qin, Y.Y., Gong, W., Zhang, Y.J., Kong, X., et al. (2016). Long Noncoding RNA GCASPC, a Target of miR-17-3p, Negatively Regulates Pyruvate Carboxylase-Dependent Cell Proliferation in Gallbladder Cancer. Cancer Res. *76*, 5361–5371.
42. Hou, W., Song, L., Zhao, Y., Liu, Q., and Zhang, S. (2017). Inhibition of Beclin-1-Mediated Autophagy by MicroRNA-17-5p Enhanced the Radiosensitivity of Glioma Cells. Oncol. Res. *25*, 43–53.
43. Leung, C.M., Chen, T.W., Li, S.C., Ho, M.R., Hu, L.Y., Liu, W.S., Wu, T.T., Hsu, P.C., Chang, H.T., and Tsai, K.W. (2014). MicroRNA expression profiles in human breast cancer cells after multifraction and single-dose radiation treatment. Oncol. Rep. *31*, 2147–2156.
44. Chaudhry, M.A., and Omaruddin, R.A. (2012). Differential regulation of microRNA expression in irradiated and bystander cells. Mol. Biol. (Mosk.) *46*, 634–643.

45. Chaudhry, M.A., Sachdeva, H., and Omaruddin, R.A. (2010). Radiation-induced micro-RNA modulation in glioblastoma cells differing in DNA-repair pathways. DNA Cell Biol. *29*, 553–561.

46. Curti, V., Capelli, E., Boschi, F., Nabavi, S.F., Bongiorno, A.I., Habtemariam, S., Nabavi, S.M., and Daglia, M. (2014). Modulation of human miR-17-3p expression by methyl 3-O-methyl gallate as explanation of its in vivo protective activities. Mol. Nutr. Food Res. *58*, 1776–1784.

47. Tian, B., Maidana, D.E., Dib, B., Miller, J.B., Bouzika, P., Miller, J.W., Vavvas, D.G., and Lin, H. (2016). miR-17-3p Exacerbates Oxidative Damage in Human Retinal Pigment Epithelial Cells. PLoS ONE *11*, e0160887.

48. Curti, V., Di Lorenzo, A., Rossi, D., Martino, E., Capelli, E., Collina, S., and Daglia, M. (2017). Enantioselective Modulatory Effects of Naringenin Enantiomers on the Expression Levels of miR-17-3p Involved in Endogenous Antioxidant Defenses. Nutrients *9*, E215.

49. Yuan, X.H., Fan, Y.Y., Yang, C.R., Gao, X.R., Zhang, L.L., Hu, Y., Wang, Y.Q., and Jun, H. (2016). Progesterone amplifies oxidative stress signal and promotes NO production via H_2O_2 in mouse kidney arterial endothelial cells. J. Steroid Biochem. Mol. Biol. *155* (Pt A), 104–111.

50. Park, S.J., Kim, H.B., Piao, C., Kang, M.Y., Park, S.G., Kim, S.W., and Lee, J.H. (2017). p53R2 regulates thioredoxin reductase activity through interaction with TrxR2. Biochem. Biophys. Res. Commun. *482*, 706–712.

OMTN, Volume *13*

Supplemental Information

miR-17-3p Downregulates Mitochondrial Antioxidant Enzymes and Enhances the Radiosensitivity of Prostate Cancer Cells

Zhi Xu, Yanyan Zhang, Jiaji Ding, Weizi Hu, Chunli Tan, Mei Wang, Jinhai Tang, and Yong Xu

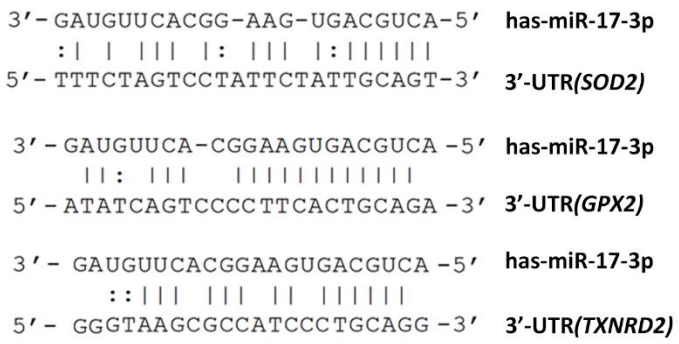

Figure S1. The putative binding sites of miR-17-3p located in the 3'-UTR of the three antioxidant genes. The *SOD2* gene encodes manganese superoxide dismutase (MnSOD), a primary antioxidant enzyme in mitochondria; the *GPX2* gene encodes glutathione peroxidase 2 (Gpx2) in mitochondria; the *TXNRD2* gene encodes thioredoxin reductase 2 (TrxR2) in mitochondria.

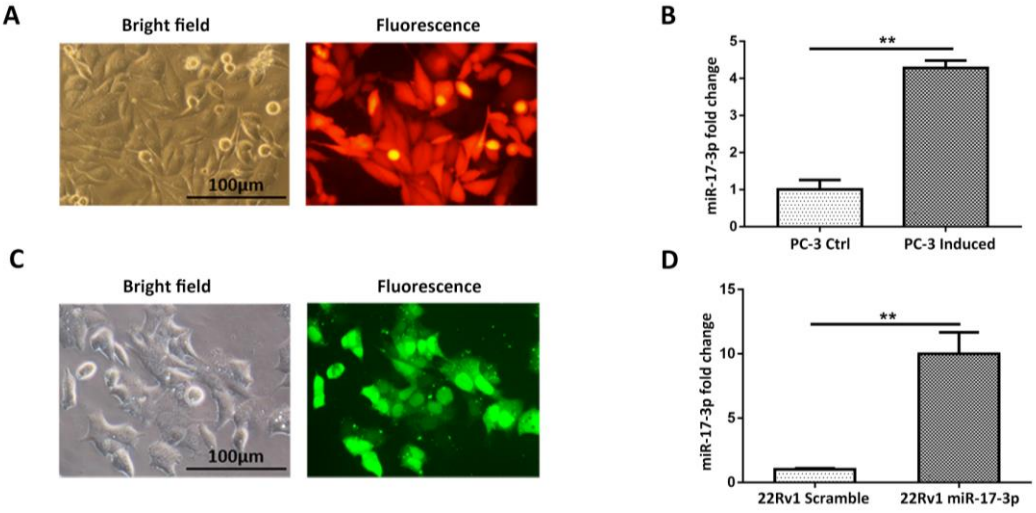

Figure S2. Ectopically expressed miR-17-3p in PCa cells. (A) A Tet-on regulated lentiviral expressing miR-17-3p was stably transducted into PC-3 cells and validated by Dox inducer. The expression of RFP-tag was determined. (B) The levels of miR-17-3p in Dox-induced cells were quantified by qRT-PCR. (C) miR-17-3p was transfected into 22Rv1 cells and screened by green fluorescence. (D) The levels of miR-17-3p in 22Rv1 cells were quantified by qRT-PCR. **($P< 0.01$) present the significances between two groups.

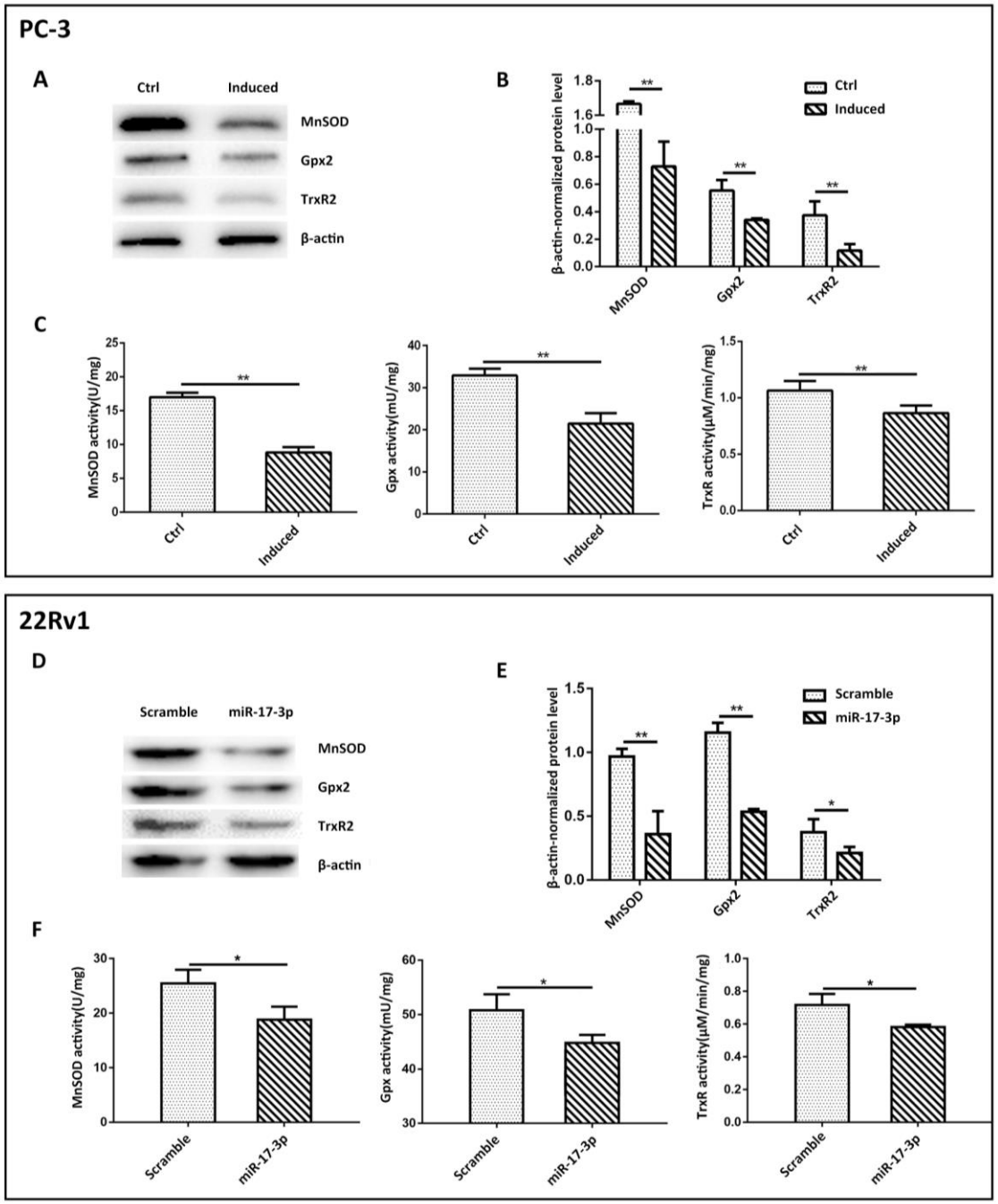

Figure S3. Quantification of MnSOD, Gpx and TrxR in the miR-17-3p expressed cells. (A and B) After Dox treatment, the PC-3 cell extracts were used to quantify the three antioxidant enzymes by western blots. (C) The relating enzymatic activities of the three antioxidant enzymes were measured accordingly. (D-F) After transfecting miR-17-3p into 22Rv1 cells, the protein levels of the three antioxidant enzymes and their activities were quantified corresponding to A-C. NS, not significant, *($P<0.05$) and **($P< 0.01$) present the significances between two groups.

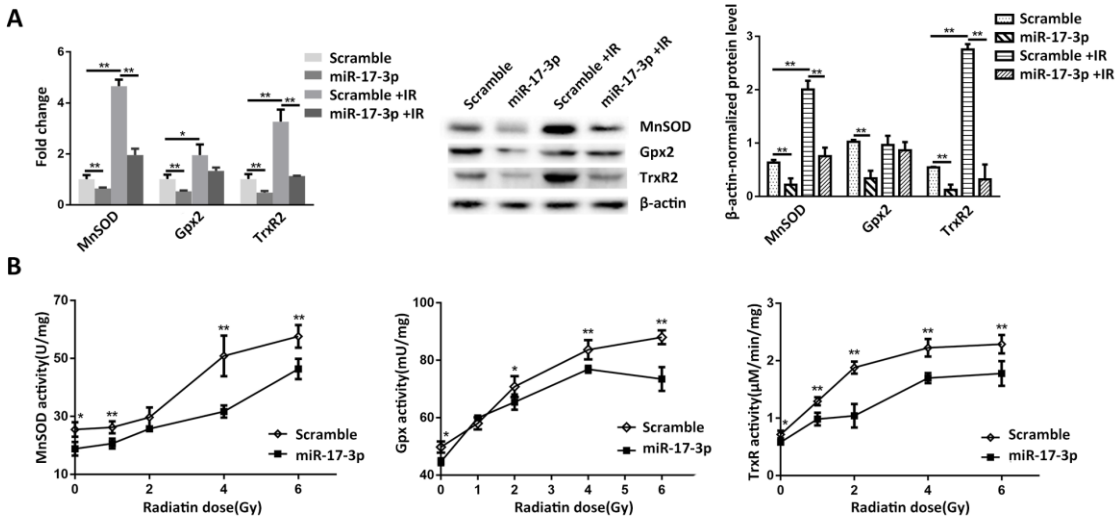

Figure S4. miR-17-3p-medicated suppression of IR-induced three mitochondrial antioxidants in 22Rv1 cells. (A) The miR-17-3p transfected cells were treated with IR and the expression levels of the three antioxidant enzymes were determined by qRT-PCR and western blots with β-actin normalization. (B) After miR-17-3p transfection, the cells were treated with different doses of IR as indicated. The enzymatic activities of the three antioxidant enzymes were measured. *(P<0.05) and **(P< 0.01) present the significances between two groups.

Table S1

The sequences of quantitive PCR primers

miR-17-3p	Forward: CCTCAATTGATTCACCCACC
	Reverse: GCTGCTCTCCCCAAGGAT
SOD2	Forward: AGCATGTTGAGCCGGGCAGT
	Reverse: AGGTTGTTCACGTAGGCCGC
GPX2	Forward: TGGTGGCCTGTGTCTGTAGT
	Reverse: TCAGGATCTCCTCATTCTGACA
TXNRD2	Forward: CAGCGGGACTATGATCTCCT
	Reverse: AGGTTCCACGTAGTCCACCA
β-actin	Forward: CCTCAATTGATTCACCCACC
	Reverse: GCTGCTCTCCCCAAGGAT